RESEARCH ARTICLE

Bi$_2$O$_3$ ISLANDS ON NANOCOMPOSITE Zr$_{(0.25)}$Sn$_{(0.75)}$O$_4$ SURFACE ACT AS THE PPM LEVEL H$_2$S GAS MONITOR WORKING AT ROOM TEMPERATURE

G. B. Shelke

Associate Professor, Dept. of Physics, Nanasaheb Y. N. Chavan College, Chalisgaon, MS, India, 424101.

………………………………………………………………………………………………....

Manuscript Info	*Abstract*

………………………….   ………………………………………………………

Bulk ZrO$_2$ and SnO$_2$ powders were separately synthesized by disc type ultrasonicated microwave assisted followed centrifuge technique. Synthesized powders of bulk SnO$_2$ and ZrO$_2$ are not exactly stoichiometric and hence not insulating. Nanocomposite material, Zr$_{(0.25)}$Sn$_{(0.75)}$O$_4$ was prepared by using synthesized ZrO$_2$ and SnO$_2$ powders by taking their 1:3 proportion. Thick films of nanostructured pure Zr$_{(0.25)}$Sn$_{(0.75)}$O$_4$ powder were fabricated by screen printing technique. These films were surface activated by dipping technique using bismuth oxide (Bi$_2$O$_3$) for different intervals of time, viz. 5 min, 15 min, 30 min and 45 min followed by firing at 450°C for 30 min. It was observed that, the 15 min Bi$_2$O$_3$ activated Zr$_{(0.25)}$Sn$_{(0.75)}$O$_4$ thick film is most sensitive to 5 ppm H$_2$S gas at room temperature.The average crystallite size was observed to be of 8.1 nm and determined using Scherer's formula. Characterization techniques such as X-Ray diffraction studies (XRD), Field effect scanning electron microscopy (FESEM), Energy dispersive analysis (EDAX) by X rays, etc. were employed to study the average particle size, surface morphology and elemental analysis of the nanocomposite. The gas response, selectivity, response and recovery times of the sensor in the presence of H$_2$S and other gases were studied and discussed.

………………………………………………………………………………………………....

Introduction:-

The technological progress made by mankind has changed and shaped the world. But, this progress has several side effects, major being related to the environment. The industrial development all over the world is generating toxic solid, liquid and gaseous wastes. The hazardous gases like CO, NO$_x$, Cl$_2$, NH$_3$, H$_2$S, etc. are polluting the air blanket of the earth which is creating several health issues for the human beings. The health issues include several diseases like respiratory track diseases, viz. bronchitis, asthma, nausea, shortness of breath, lung cancer, reduction in hemoglobin, impairment of nervous system, mental retardation, disorders of digestive system, blindness, reproductive system, hypertension, forgetfulness, headaches, etc. (Brooks M., et al. 1998; Durham W. B., 1978; Eckerman I., 1984; Heylin M., 1994; Gupta B. N., et al. 1988; Kuanr B. K., et al. 2008; Kirsi Kuoppamaki, et al. 2014).

Therefore, it is today's need to keep watch and monitor the air quality with the help of gas sensors. Such monitoring can be made outdoors as well as indoors. The detection of gas pollution with the help of sensors can help in the elimination of these polluting gases and thus improve an air quality. These gas sensors can be seen as security

Corresponding Author:- G. B. Shelke
Address:- Associate Professor, Dept. of Physics, Nanasaheb Y. N. Chavan College, Chalisgaon, MS, India, 424101.

equipments for environmental security. The pollutant gases are of various types and they originate in different physical conditions like temperature, radiations, etc. (Marilena Kampa, et al. 2008; Air Quality Guidelines for Europe 2000; Cullis C. F., et al. 1989; Patil D. R., 2011; Moore P. D., 1995; Dasmann R. F., 1976).

A lot of research and development is in progress to design portable and affordable gas sensors which possess highest response, producing ability at trace levels of gaseous species, selective nature among mixture of various gases, long term stability, low cost, large applicability, etc. (Shelke G. B., 2019). The aim of the present work is, to fabricate and develop the gas sensors by utilizing the pure and surface activated nanocomposites, $Zr_{(1-x)}Sn_{(x)}O_4$ so that, they could be able to detect various gas traces at ppm / ppb level.

Experimental Procedure:-
Synthesis of Powders, Thick Film Fabrication and Surface Activation:
$Zr_{1-x}Sn_xO_4$ nanocomposites in the form of dry powders were synthesized by disc type ultrasonicated microwave treatment followed centrifuge technique (Gawas U. B., et al. 2011; Shelke G. B., et al. 2019; Khamkar K. A., et al. 2012), by hydrolysis of AR grade zirconium oxychloride and tin chloride in aqueous-alcohol solution. Initially, aqueous-alcohol solution was prepared from distilled water and propylene glycol in the ratio of 1:1. The prepared solution was then mixed with 1M aqueous solution of zirconium oxychloride and tin chloride in the desired proportions. The special arrangement was made to add drop wise aqueous ammonia at the rate of 0.1 ml / min with constant stirring until the optimum pH of solutions become in the range from 7.9 to 10.8, varies for various concentrations of dopant. After complete precipitation and centrifugation, the hydroxide was washed with distilled water until chloride ions were not detected by $AgNO_3$ solution. Then, the precipitates were allowed for ultrasonication and then placed in a microwave oven for 10 minutes with continuous on-off cycles, periodically, followed by calcination at 500ºC for 2 hrs. in muffle furnace. The dried precipitates were ground by agate pestle-mortar to ensure sufficiently fine particle size and re-calcined in a muffle furnace at 500°C for 2 hrs., to eliminate the organic impurities, if present. Thus, the dry powders of nanostructured $Zr_{(0.25)}Sn_{(0.75)}O_4$ have been prepared and ready to use.

The thixotropic paste was formulated by mixing the synthesized $Zr_{(0.25)}Sn_{(0.75)}O_4$ fine powder with a temporary binder as explained elsewhere (Bagal L. K., et al. 2012; Patil D. R., et al. 2007; Patil D. R., et al. 2006). This thixotropic paste was then screen printed on a glass substrate in the form of desired sized rectangular patterns. The films prepared were fired at 500ºC for 30 min. Thus, the thick films of pure $Zr_{(0.25)}Sn_{(0.75)}O_4$ are now ready to use for the surface activation process.

The screen printed thick films were activated by dipping them into 0.01 M aqueous solutions of bismuth chloride for different intervals of time, viz. 5 min, 15 min, 30 min and 45 min and dried at 80ºC under an IR lamp, followed by firing at 500ºC for 30 min in an ambient air. The particles of bismuth chloride dispersed on the film surface would be transformed to bismuth oxide (Bi_2O_3), upon firing process. Sensor elements with different mass percentage of Bi_2O_3 incorporated in to thick films of pure $Zr_{(0.25)}Sn_{(0.75)}O_4$ were prepared. Hence, Bi_2O_3 islands of different concentrations formed on the pure nanocomposite thick films. Silver contacts were made by vacuum evaporation for electrical measurements and monitoring the gas sensing performance of the thick films (Shelke G. B., et al. 2017).

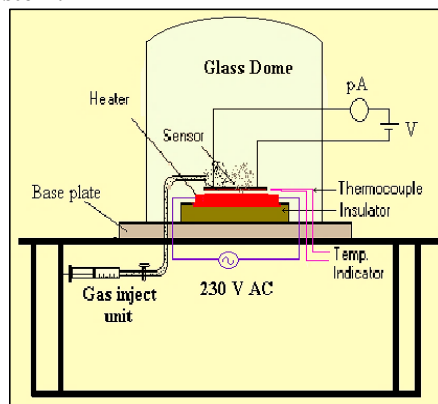**Details of the Static Gas Sensing System:**

Fig. 1:- Block diagram of static gas sensing system

Fig. 1 shows the block diagram of the static gas sensing system. The sensor element, heating unit, dc power supply, gas inject unit, temperature measuring unit, current meter (pico-ammeter), glass dome and steel base plate are the major components of static gas sensing system. The static gas sensing system is built in the laboratory. Heating unit is fixed on the base plate. It provides the desired temperature to sensor for its proper performance. Sample to test of prepared thick film was mounted 2 to 3 cm above the heater. Cr-Al thermocouple is mounted to measure the temperature. The output of thermocouple is connected to the temperature indicator. Inlet gas port was fitted at one of the ports of base plate. Gas concentration inside the static system is achieved by injecting a known volume of test gas by gas inject syringe. A constant d. c. 30 V is applied to the sensor element and the current is measured by means of pico-ammeter, for the measurement of I-V characteristics. Air was allowed to pass into the glass dome after every H_2S gas exposure cycle.

Results and Discussion:-
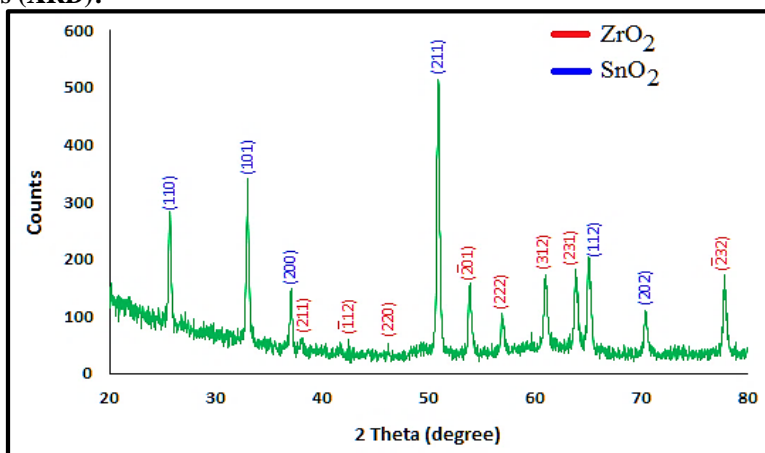**Material's Characterizations:**
Structural Properties (XRD):

Fig. 2:- XRD of pure $Zr_{(0.25)}Sn_{(0.75)}O_4$ powder

Fig. 2 depicts the X-ray diffractogram of pure $Zr_{(0.25)}Sn_{(0.75)}O_4$ powder. The 2θ peaks observed are correspond to the (110), (101), (200), (211), ($\bar{1}$12), (220), (211), ($\bar{2}$01), (222), (312), (231), (112), (202) and ($\bar{2}$32) planes of reflections. No peaks corresponding to Bi_2O_3 were observed in XRD pattern of surface activated thick films, which may be due to their very small mass % dispersed on the surface of $Zr_{(0.25)}Sn_{(0.75)}O_4$ film. The XRD spectrum reveals that, the material is poly-nano-crystalline in nature and combination of tetragonal-monoclinic in structure. The observed peaks are matching well with JCPDS reported data of pure SnO_2-ZrO_2. The average crystallite size was observed to be of 8.1 nm and determined by using Scherer's formula.

Energy Dispersive Analysis by X-Rays (E-DAX):
Table 1:- Elemental analysis of pure and Bi_2O_3 activated $Zr_{(0.25)}Sn_{(0.75)}O_4$ thick films

Mass %	Activation Time (min)					
	0 (Pure) (Expected)	0 (Pure) (Observed)	5	15	30	45
O	36.40	24.72	21.95	08.23	09.82	09.71
Zr	12.97	21.30	05.07	07.98	10.08	05.62
Sn	50.63	53.98	62.78	60.45	38.68	19.36
$Zr_{(0.25)}Sn_{(0.75)}O_4$	100	100	88.63	73.82	53.82	27.19
Bi	00	00	10.20	23.35	41.42	65.31
Bi_2O_3	00	00	11.37	26.18	46.18	72.81
Bi_2O_3 + $Zr_{(0.25)}Sn_{(0.75)}O_4$	100	100	100	100	100	100

The quantitative elemental composition of the pure $Zr_{(0.25)}Sn_{(0.75)}O_4$ and Bi_2O_3 activated $Zr_{(0.25)}Sn_{(0.75)}O_4$ thick films were analyzed using an energy dispersive spectrometer and mass % of O, Zr, Sn, $Zr_{(0.25)}Sn_{(0.75)}O_4$, Bi, Bi_2O_3 and

$Bi_2O_3+Zr_{(0.25)}Sn_{(0.75)}O_4$ are represented in Table 1. The prepared powder of pure $Zr_{(0.25)}Sn_{(0.75)}O_4$ is deficient in oxygen, which increases its n-typeness characteristic. This leads to n-type semiconducting nature of the synthesized $Zr_{(0.25)}Sn_{(0.75)}O_4$. Also, the mass % of Zr, Sn and O in each activated samples are not as per the stoichiometric proportion and all the samples are observed to be oxygen deficient. This enhances n-typeness of activated $Zr_{(0.25)}Sn_{(0.75)}O_4$ thick films.

Microstructural Analysis (FESEM):
Pure $Zr_{(0.25)}Sn_{(0.75)}O_4$:
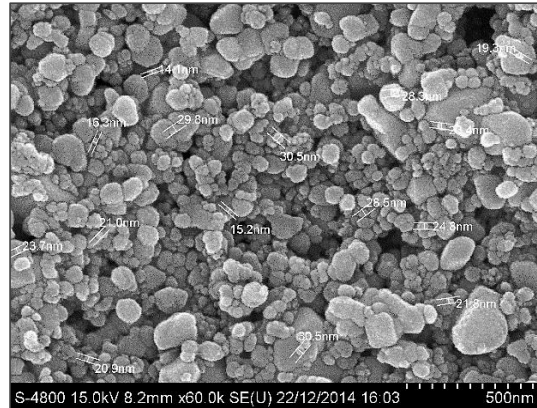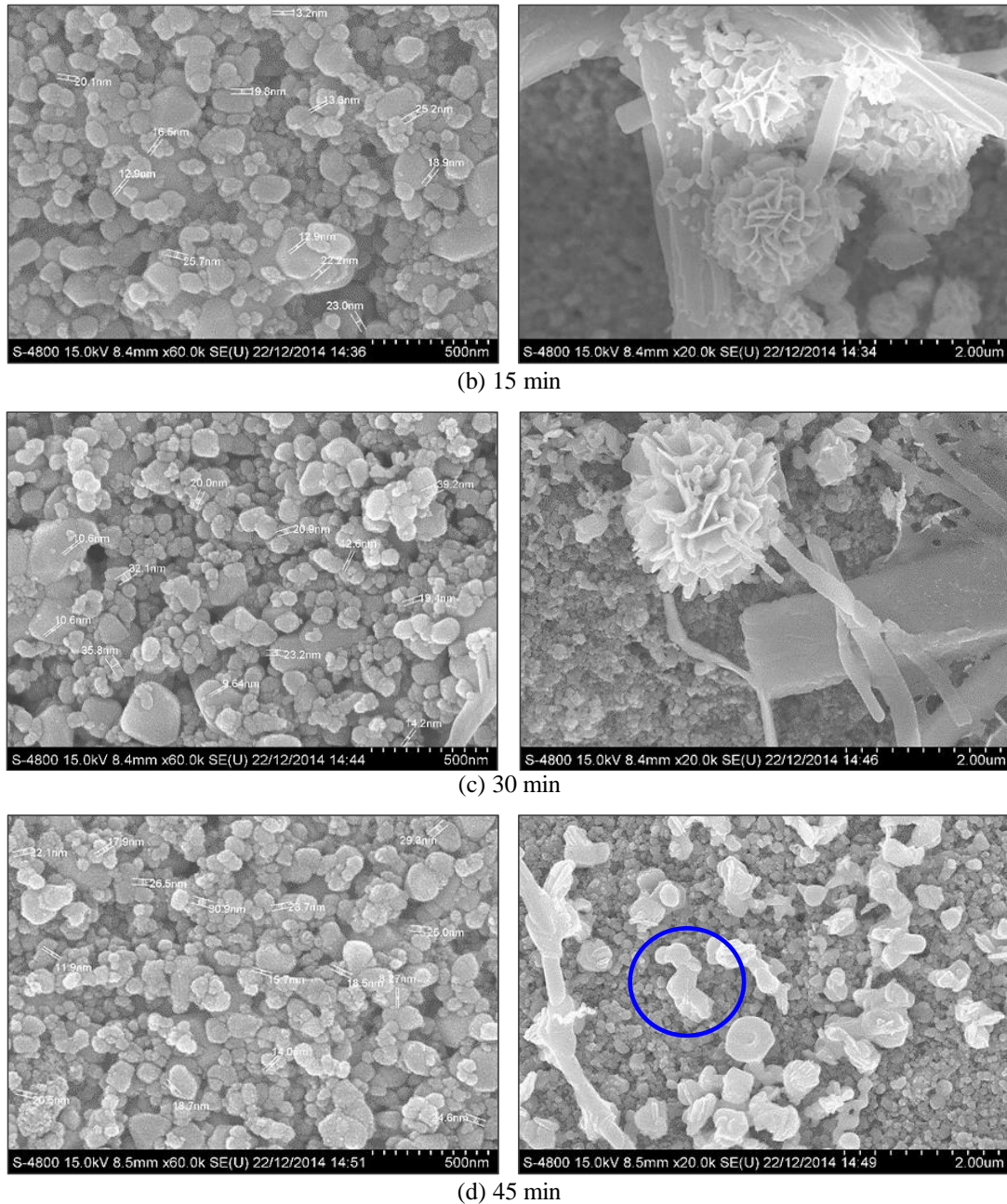

Fig. 3:- Micrograph of pure $Zr_{(0.25)}Sn_{(0.75)}O_4$ thick film

Fig. 3 depicts the SEM image of pure $Zr_{(0.25)}Sn_{(0.75)}O_4$ thick film fired at 500ºC for 30 min, which consists of voids and a wide range of randomly distributed grains with sizes ranging from 10 nm to 30 nm. The film has porous nature, which supports the adsorption-desorption type of gas sensing mechanism. The nanoscaled grains exhibit high surface to volume ratio. The less numbers of smaller grains of zirconium oxide are fused with the large numbers of larger grains of tin oxide (Shelke G. B., 2020).

Bi_2O_3 Activated $Zr_{(0.25)}Sn_{(0.75)}O_4$:

(a) 5 min
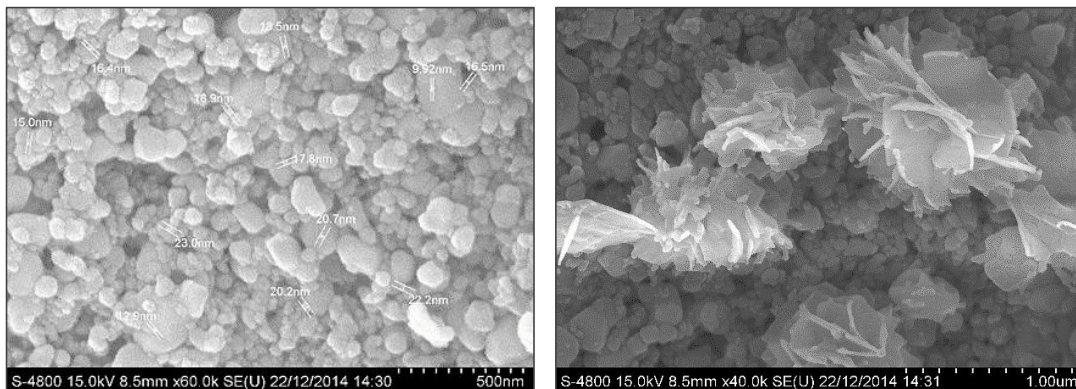
(b) 15 min

(c) 30 min

(d) 45 min

Fig. 4:- Micrographs of Bi$_2$O$_3$ activated Zr$_{(0.25)}$Sn$_{(0.75)}$O$_4$ thick films

Figs. 4 (a to d) depict the microstructures of Bi$_2$O$_3$ activated Zr$_{(0.25)}$Sn$_{(0.75)}$O$_4$ thick films for various activation time, viz. 5 min, 15 min, 30 min and 45 min and at two magnifications, each.

Fig. 4 (a) depicts the fabrication of Bi$_2$O$_3$ nano-petals on the surface of Zr$_{(0.25)}$Sn$_{(0.75)}$O$_4$ film, further forming nanoflowers. The thickness of nano-petals is about 20-30 nm. The voids, nano-petals and nanoflowers are randomly distributed and even oriented on the film surface.

Fig. 4 (b) depicts the fabrication of Bi$_2$O$_3$ nanosheets, nanopetals and nanoflowers on the Zr$_{(0.25)}$Sn$_{(0.75)}$O$_4$ film surface, distributed randomly with voids. The average size of Bi$_2$O$_3$ nanosheets is about 60 nm and that of the nano-petals is about 30 nm. This film was observed to be the most sensitive to trace level H$_2$S gas at room temperature. The high performance of this film in gas sensing may be attributed to the enhancement of active surface to volume

237

ratio due to nanoflower like porous structure. So, the large surface active sites are available to reach the gas molecules to the interstitials of the film. Therefore, large numbers of free electrons are made available during the gas exposure and its oxidation. The activated film surfaces at a certain level would enhance the gas sensing performance of the films. This may help in oxidizing the target gas quickly.

Fig. 4 (c) depicts the nanosheets, nano-petals and nanoflowers of Bi_2O_3 on the $Zr_{(0.25)}Sn_{(0.75)}O_4$ film surface. Film consists of voids and random distribution of nanosheets, nano-petals and nanoflowers on the film surface. The average size of Bi_2O_3 nanosheets is about 25 nm and the thickness of nano-petals is about 20 nm.

Fig. 4 (d) depicts the formation of nanosheets and nanoflowers of Bi_2O_3 on the $Zr_{(0.25)}Sn_{(0.75)}O_4$ film surface. The marked region on the image shows the formation of nanopetals of a nanoflower. It is clear from figures that, with the increase of activation time, there is a change in the texture of the films. Larger the activation time, larger would be the amount of Bi_2O_3 dispersed on the surface, and smaller would be the chances of reaching the gas to interstitial sites of the material. The activation time was therefore optimized to have optimum number of Bi_2O_3 misfits dispersed uniformly on the surface to utilize it for the gas sensing mechanism.
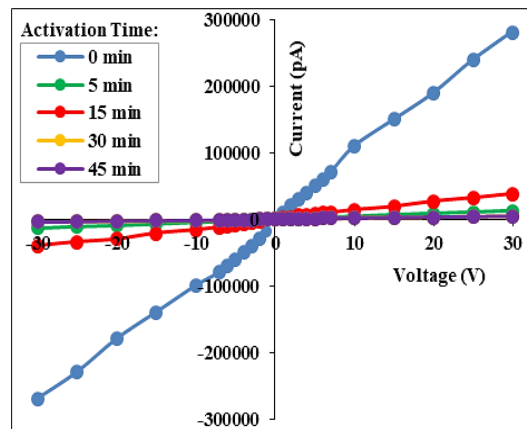
Electrical Performance:
I-V Characteristics:

Fig. 5:- I-V characteristics

Fig. 5 depict the I-V characteristics of pure and Bi_2O_3 activated $Zr_{(0.25)}Sn_{(0.75)}O_4$ thick films. It is clear from the symmetrical nature of I-V characteristics that, the materials as well as silver contacts made on the films for external connections, are ohmic in nature. The materials are therefore said to have possessing the resistive properties, though more or less.
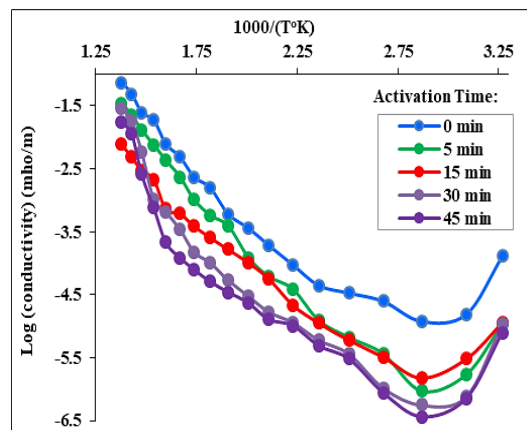
Electrical Conductivity:

Fig. 6:- Conductivity profile

Fig. 6 depict the variation of log of conductivity with the reciprocal of operating temperature of Bi_2O_3 activated $Zr_{(0.25)}Sn_{(0.75)}O_4$ thick films. The conductivities of all the samples are minimum at 75°C operating temperature. It was found that, all the pure and activated films exhibit the lowest conductivities in the temperature range from 100°C to 75°C. This is the temperature range in which all the films exhibit insulating nature, above which the films exhibit NTC and below it, the films exhibit PTC nature. Thus the material switches its semiconducting nature from NTC to PTC through insulating nature, with decrease in temperature from 400°C to room temperature (32°C). Hence, one should not expect the application of this material in the field of gas sensing.

Gas Sensing Performance of the Sensors:
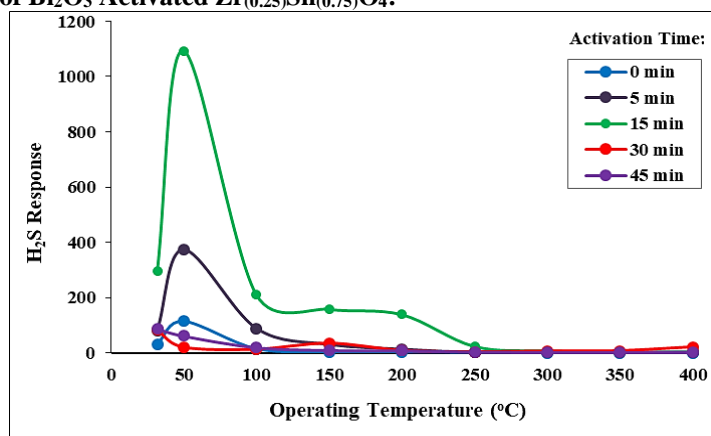**Gas Sensing Response of Bi_2O_3 Activated $Zr_{(0.25)}Sn_{(0.75)}O_4$:**

Fig. 7:- H_2S response

Fig. 7 depicts the variation of 5 ppm H_2S gas response with operating temperature of pure and Bi_2O_3 activated $Zr_{(0.25)}Sn_{(0.75)}O_4$ thick films. It is clear from figure that, Bi_2O_3 activated $Zr_{(0.25)}Sn_{(0.75)}O_4$ thick film at 15 min activation time exhibits crucial response to 5 ppm H_2S gas at room temperature (32°C) as well as at 50°C. From elemental analysis, it was observed that, the Bi_2O_3 activated $Zr_{(0.25)}Sn_{(0.75)}O_4$ (15 min) thick film is observed to be the most oxygen deficient. This enhances n-typeness of activated $Zr_{(0.25)}Sn_{(0.75)}O_4$. During surface activation of the film, Bi_2O_3-$Zr_{(0.25)}Sn_{(0.75)}O_4$ heterostructures were formed on the surface of the film, decreasing the conductivity of the activated film. Upon exposure, H_2S gas gets oxidized by utilizing the lattice oxygen from the surface at room temperature, trapping behind the free electrons in the material and enhances the conductivity of the material. This may be the reason of increase in conductivity of the sensor upon exposure of H_2S gas at the room temperature. But, as the temperature increases, the H_2S response increases up to 50°C, and then decreases further with operating temperature.

Active Nature:

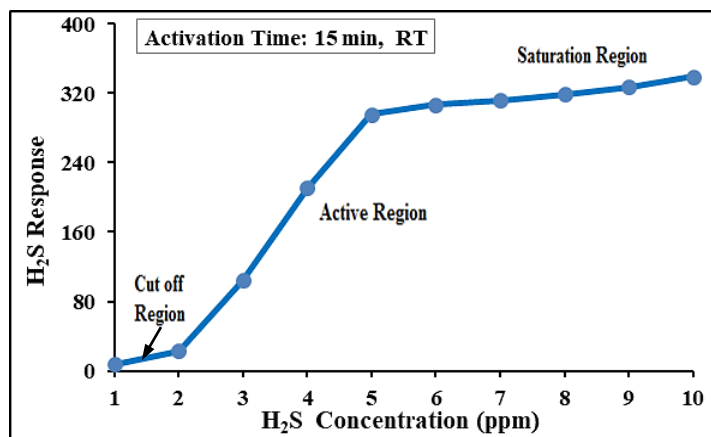**Fig. 8:-** Variation in H_2S response with H_2S gas concentration (ppm)

The variation of H_2S response of pure and Bi_2O_3 activated $Zr_{(0.25)}Sn_{(0.75)}O_4$ thick films with H_2S gas concentration at room temperature, are represented in Fig. 8. It is clear from the figure that; the gas response goes on increasing linearly with gas concentration up to 5 ppm. The rate of increase in H_2S response was relatively larger up to 5 ppm and saturated beyond 5 ppm. Thus, the active region of the sensor would be up to 5 ppm.
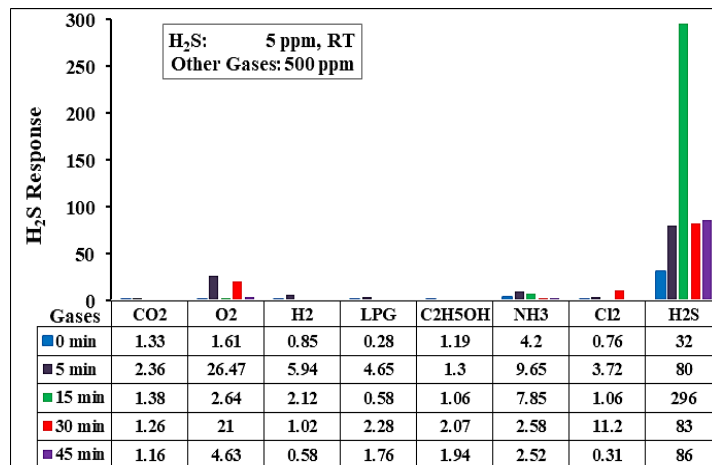
Selective Nature:

Gases	CO2	O2	H2	LPG	C2H5OH	NH3	Cl2	H2S
0 min	1.33	1.61	0.85	0.28	1.19	4.2	0.76	32
5 min	2.36	26.47	5.94	4.65	1.3	9.65	3.72	80
15 min	1.38	2.64	2.12	0.58	1.06	7.85	1.06	296
30 min	1.26	21	1.02	2.28	2.07	2.58	11.2	83
45 min	1.16	4.63	0.58	1.76	1.94	2.52	0.31	86

Fig. 9:- Selective nature

It is observed from Fig. 9 that, the 15 min Bi_2O_3 activated $Zr_{(0.25)}Sn_{(0.75)}O_4$ thick film is most sensitive to 5 ppm H_2S at room temperature. This is the optimized condition for surface activation of $Zr_{(0.25)}Sn_{(0.75)}O_4$ with the help of Bi_2O_3. Also, it has high selectivity against different gases, viz. CO_2, O_2, H_2, LPG, C_2H_5OH, NH_3 and Cl_2.

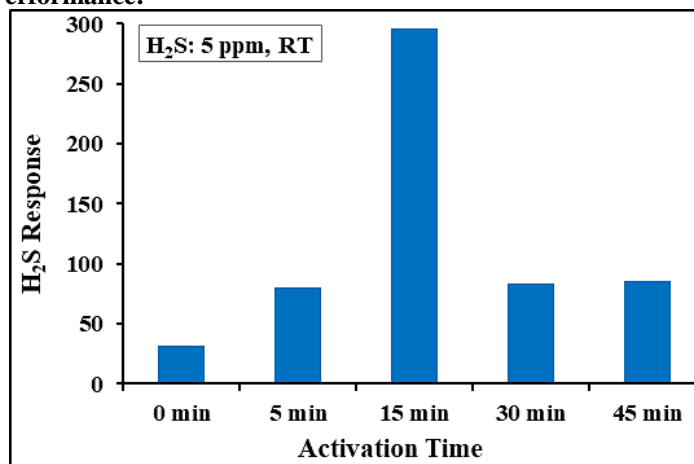**Activation Dependent Performance:**

Fig. 10: Variation of H_2S response with activation time (min)

Fig. 10 indicates the H_2S response as a function of the activation time of the Bi_2O_3 activated $Zr_{(0.25)}Sn_{(0.75)}O_4$ thick film sensor. The pure $Zr_{(0.25)}Sn_{(0.75)}O_4$ thick film was observed to be less sensitive to trace level of H_2S at room temperature and at higher temperature range. The activation of thick films of pure $Zr_{(0.25)}Sn_{(0.75)}O_4$ by Bi_2O_3 enhances the H_2S response. It was observed that, the response to H_2S increases with activation time, reaches to maximum at 15 min and then falls down even with increase in the activation time. The film activated for 15 min was observed to be the most sensitive to H_2S at room temperature.

Long Term Stable Nature:
Fig. 11 indicates the H_2S response over a long time duration for the Bi_2O_3 activated $Zr_{(0.25)}Sn_{(0.75)}O_4$ (15 min) thick film sensor. The sensor was observed to be the most sensitive to H_2S at room temperature. The sensor response to

H$_2$S was observed to be constant over a long duration (few months). It was observed that, the sensor response decreases by about 10 % after 40 days, and remains same thereafter.
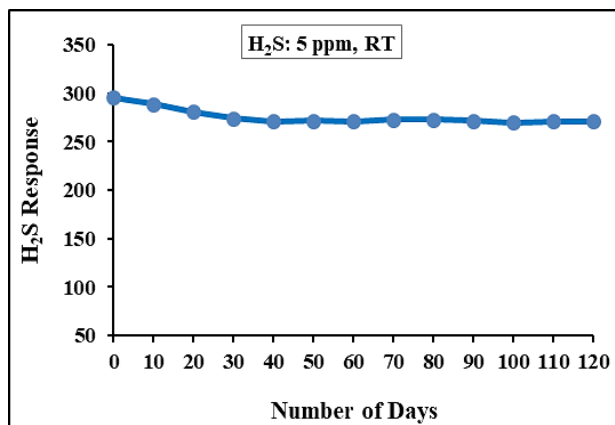

Fig. 11:- H$_2$S response over long time duration (Days)
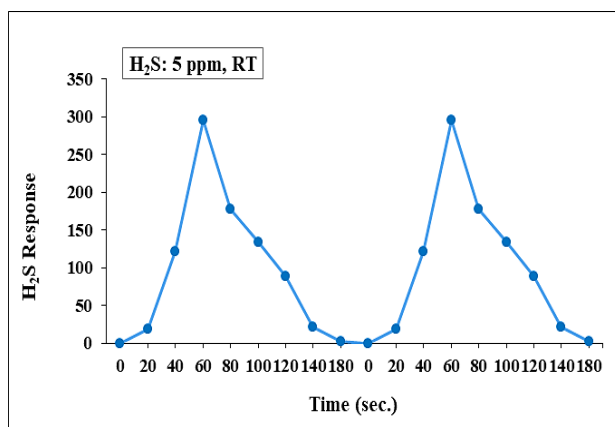
Response - Recovery Nature:

Fig. 12:- Response and recovery of Bi$_2$O$_3$ activated Zr$_{(0.25)}$Sn$_{(0.75)}$O$_4$ thick film

The response and recovery of the Bi$_2$O$_3$ activated Zr$_{(0.25)}$Sn$_{(0.75)}$O$_4$ (15 min) thick film sensor is represented in Fig. 12. The response time of the sensor was of the order of 50 sec. to 5 ppm of H$_2$S gas and recovery time is of the order of 80 sec. For better performance of the sensor, the recovery should be very fast. When the gas exposure was switched off, the sensor returned back to its original chemical status, within 80 sec.

Conclusions:-
From the results obtained, the following statements can be made for the sensing performance of Bi$_2$O$_3$ activated Zr$_{(0.25)}$Sn$_{(0.75)}$O$_4$ sensors.
1. Pure Zr$_{(0.25)}$Sn$_{(0.75)}$O$_4$ thick films were almost insensitive or less sensitive to hazardous and toxic gases.
2. Surface properties of the films were conveniently customized by establishing the Bi$_2$O$_3$ islands on Zr$_{(0.25)}$Sn$_{(0.75)}$O$_4$ film surface using dipping technique.
3. Bi$_2$O$_3$ activated Zr$_{(0.25)}$Sn$_{(0.75)}$O$_4$ (15 min) thick film is highly sensitive to 5 ppm H$_2$S gas at room temperature.
4. Bi$_2$O$_3$ activated Zr$_{(0.25)}$Sn$_{(0.75)}$O$_4$ (15 min) thick film is highly selective to 5 ppm H$_2$S gas at room temperature.
5. The response time of the sensor was of the order of 50 sec. to 5 ppm of H$_2$S gas and recovery time is of the order of 80 sec. The recovery of this sensor is too long, which is the drawback of this sensor.
6. The excellent features of the sensor are highly sensitive, selective, low cost, portable in size and weight and long term stability.

References:-

1. Air Quality Guidelines for Europe, 2nd Ed., WHO Regional Office for Europe, Copenhagen, Denmark (2000) pp. 57-209.
2. Bagal L. K., Patil J. Y., Mulla I. S., Suryavanshi S. S., Studies on the resistive response of nickel and cerium doped SnO_2 thick films to acetone vapour, Ceramics International, (38) 2012 pp. 6171-6179.
3. Brooks M., Coghlan A., J. Indian Science, Live and let live, New Scientists (1998) pp. 46-49.
4. Cullis C. F., Hirschler M. M., Man's emissions of carbon monoxide and hydrocarbons into the atmosphere, Atmospheric Environment 23 (1989) pp. 1195–1203.
5. Dasmann R. F., Environmental conservation, (4th Ed.) John Wiley and Sons, Inc. New York (1976) pp. 310-338.
6. Durham W. B., Industrial Pollution, Sax, N. I., Van Nostrand Reinhold Co., New York (1974) pp. 10-35.
7. Eckerman I., Bhopal Gas Catastrophe 1984: Causes and Consequences, Encyclopedia of Environmental Health,(2011) pp. 302-316.
8. Gawas U. B., Verenkar V. M. S., Patil D. R., Nanostructured ferrite based electronic nose sensitive to ammonia at room temperature, Sens. Transducers, (134) 2011 pp. 45-55.
9. Gupta B. N., Rastogi S. K., Chandra H., Mathur N., Mahendra P. N., Pangtey B. S., Kumar S., Kumar P., Seth R. K., Dwivedi R. S., Ray P. K., Effect of exposure to toxic gas on the population of Bhopal: part I-epidemiological, clinical, radiological and behavioural studies, Indian J. of Experimental Biology, 26 (1988) pp. 149-160.
10. Heylin M., Bhopal: Ten years after, Chem. and Eng. News, 72 (51) (1994) pp. 18-32.
11. Khamkar K. A., Bangale S. V., Dhapte V. V., Patil D. R., Bamne S. R., A Novel Combustion Route for the Preparation of Nanocrystalline $LaAlO_3$ Oxide Based Electronic Nose Sensitive to NH_3 at Room Temperature, Sens. Transducers, (146) 2012 pp. 145-155.
12. Kirsi Kuoppamaki, Heikki Setala, Anna-Lea Rantalainen, D. Johan Kotze, Urban snow indicates pollution originating from road traffic, Environmental Pollution, 195 (2014) pp. 56-63.
13. Kuanr B. K., Maat S., Chandrashekariaih S., Veerakumar V., Camley R. E. and Celinski Z., J. Appl. Phys., 103 (2008) 07C107.
14. Marilena Kampa, Elias Castanas, Human health effects of air pollution, Environmental Pollution, 151 (2) (2008) pp. 362-367.
15. Moore P. D., Pollution: Too much of a good thing, Nature (London), 374 (1995) pp. 117-118.
16. Patil D. R., Patil L. A., Preparation and study of NH_3 gas sensing behavior of Fe_2O_3 doped ZnO thick film resistors, Sens. Transducers, (70) 2006 pp. 661-670.
17. Patil D. R., Patil L. A., Patil P. P., Cr_2O_3-activated ZnO thick film resistors for ammonia gas sensing operable at room temperature, Sens. Actuators B, (126) 2007 pp. 368–374.
18. Patil D. R., Everyman's Science, Indian Sci. Congress Association, XLVI No. 3 (2011) pp. 155-161.
19. Shelke G. B., Patil D. R., Surface functionalized $Zr_{(0.75)}Sn_{(0.25)}O_4$ by SrO_2 thick films as H_2S gas sensors, 2nd Int. Conference on Condensed Matter and Applied Physics, Bikaner, India, American Institute of Physics (AIP) Conf. Proc., (1953) 2017 pp. 030270-1 – 030270-4.
20. Shelke G. B., Ph.D. Thesis, Ch. 1, KBC North Maharashtra University Jalgaon, 2019, pp. 1-37.
21. Shelke G. B., Deshmukh G. D., Patil D. R., Synthesis and Characterizations of Nano Structured SnO_2 Thick Films and their Micro Structural Analysis, Int. J. of Current Research,11 (7) 2019 pp. 5576-5579.
22. Shelke G. B., Surface functionalized nanocomposite $Zr_{(0.25)}Sn_{(0.75)}O_4$ thick films for the detection of ppm level H_2S gas operable at room temperature, Int. J. of Creative Research Thoughts (IJCRT), 08 (04) 2020 pp. 2107-2114.